

Figure S1. Sample information and clustering annotation in primary HCC and non-tumor liver tissues. (A) Sample information sheet of HCC or HCC-adjacent tissues from six patients with HCC. (B) Violin plot, showing the detected genes across the samples after quality control. (C) UMAP plots, showing the identification of 11 clusters according to the unsupervised clustering method. (D) Dot plot, showing the marker genes expression of 11 clusters. HCC, hepatocellular carcinoma; UMAP, Unsupervised Uniform Manifold Approximation and Projection.

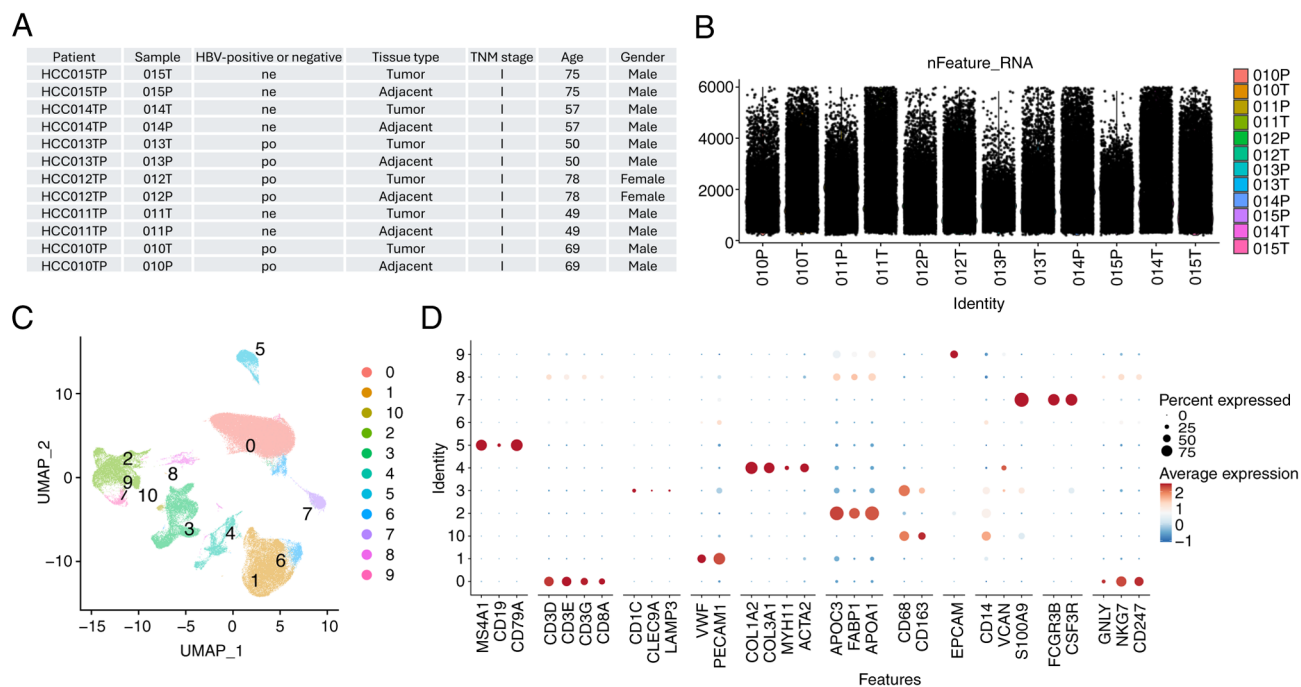


Figure S2. Changes in immune cell type proportions and *SLC35F1* expression among various types of immune cells following HBV infection. (A) Stacked bar plots, summarizing the proportions of major cell types in Ne and Po samples. (B) Dot plot, displaying the expression levels of marker genes across 13 annotated clusters. (C) Representative immunostaining images showing CD45 (red) and SLC35F1 (green) in Ne and PO hepatocellular carcinoma tissue sections. Cell nuclei were stained with DAPI (blue). The quantification is shown on the right of the panel (n=9 sections from three patients; mean \pm SEM). Statistical significance was calculated using unpaired two-tailed Student's t-test. ****P<0.0001. Scale bar, 30 μ m. HBV, hepatitis B virus; Ne, HBV-negative; Po, HBV-positive; DC, dendritic cells; NK, natural killer cells.

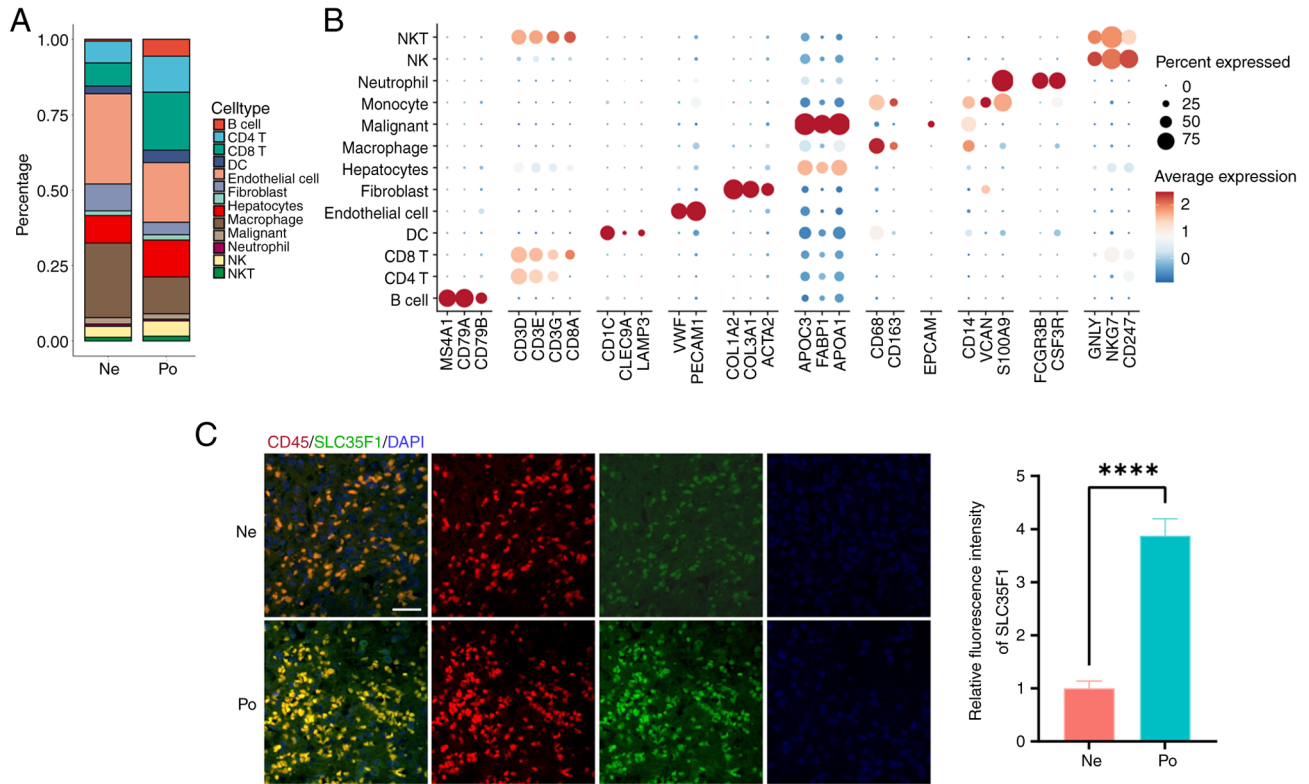


Figure S3. Pathway and functional enrichment analyses of differentially expressed genes in immune cells within HCC upon HBV infection. (A) Bar plot, showing upregulated and downregulated GO terms associated with HBV infection. (B) Dot plot, highlighting the upregulated and downregulated KEGG pathways in HBV-infected samples. (C) Gene set enrichment analysis plot, illustrating altered KEGG pathways between HBV-positive and HBV-negative samples. The P-values in (A-C) were calculated using the hypergeometric test, with Benjamini-Hochberg adjustment. HCC, hepatocellular carcinoma; HBV, hepatitis B virus; GO, Gene Ontology; Kyoto Encyclopedia of Genes and Genomes.

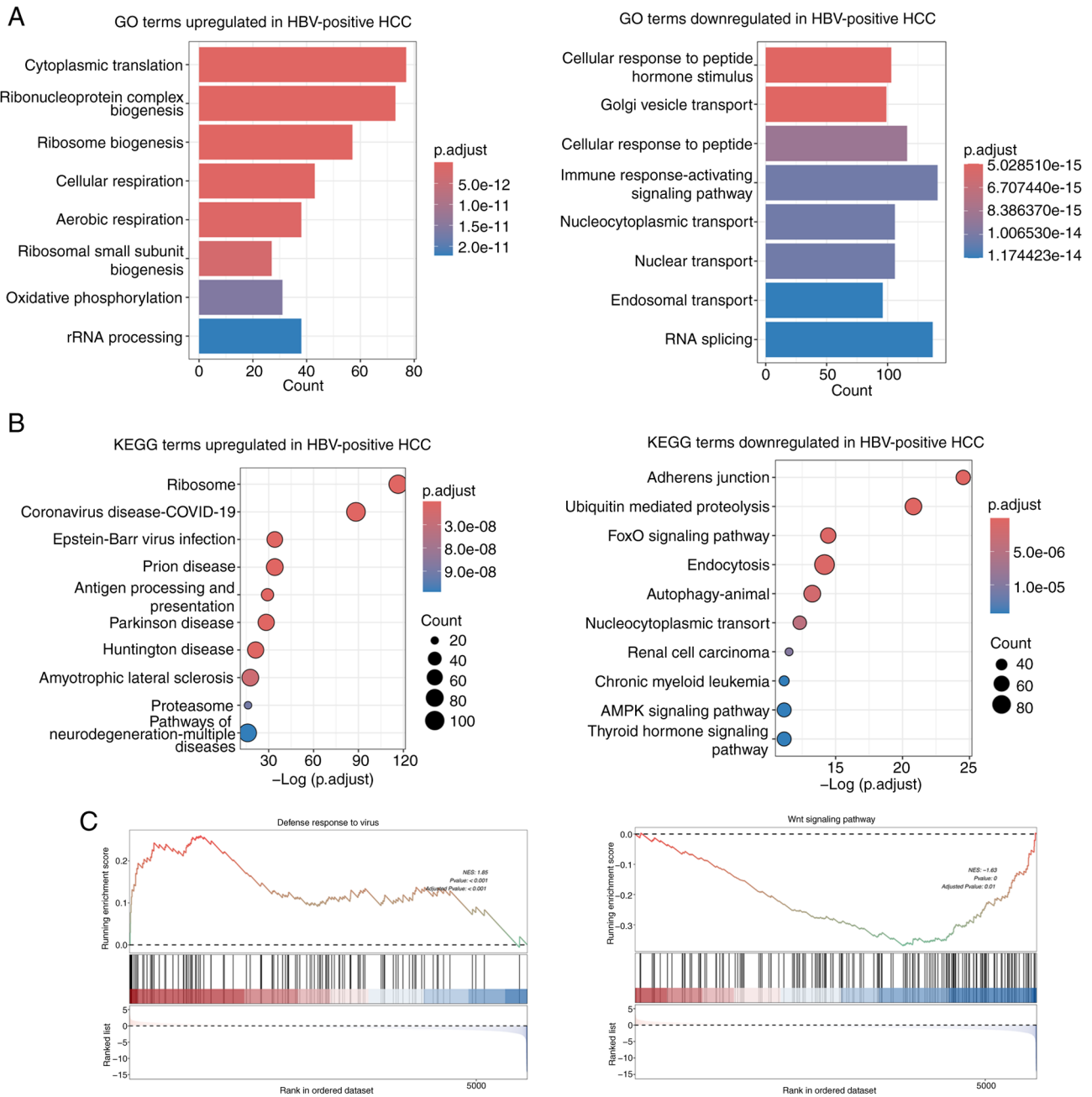


Figure S4. Proportions of immune cell subtypes across individual patients. (A) Bar plots, illustrating the distribution of CD4⁺ T cell subtypes across each sample. (B) Bar plots, depicting the distribution of CD8⁺ T cell subtypes across each sample. (C) Dot plot, displaying the percentages of cells expressing marker genes alongside their average expression levels across CD8⁺ T cell subtypes. (D) Representative images of immunostaining for CD8 (red) and SLC4A10 (green) in Ne and Po HCC tissue sections. Cell nuclei were stained with DAPI (blue). The quantification is shown on the right of the panel (n=9 sections from three patients; mean \pm SEM). (E) Bar plots, showing the proportions of macrophage subtypes across each sample. (F) Representative immunostaining images, showing CD68 (red) and IFITM3 (green) in Ne and Po HCC sections. Cell nuclei were stained with DAPI (blue). The quantification is shown on the right of the panel (n=9 sections from three patients; mean \pm SEM). (G) Bar plots presenting the proportions of DC subtypes across each sample. Statistical significance in (D and F) was calculated via unpaired two-tailed Student's t-test. *P<0.05. Scale bar, 30 μ m. HBV, hepatitis B virus; Ne, HBV-negative; Po, HBV-positive; HCC, hepatocellular carcinoma; DC, dendritic cells.

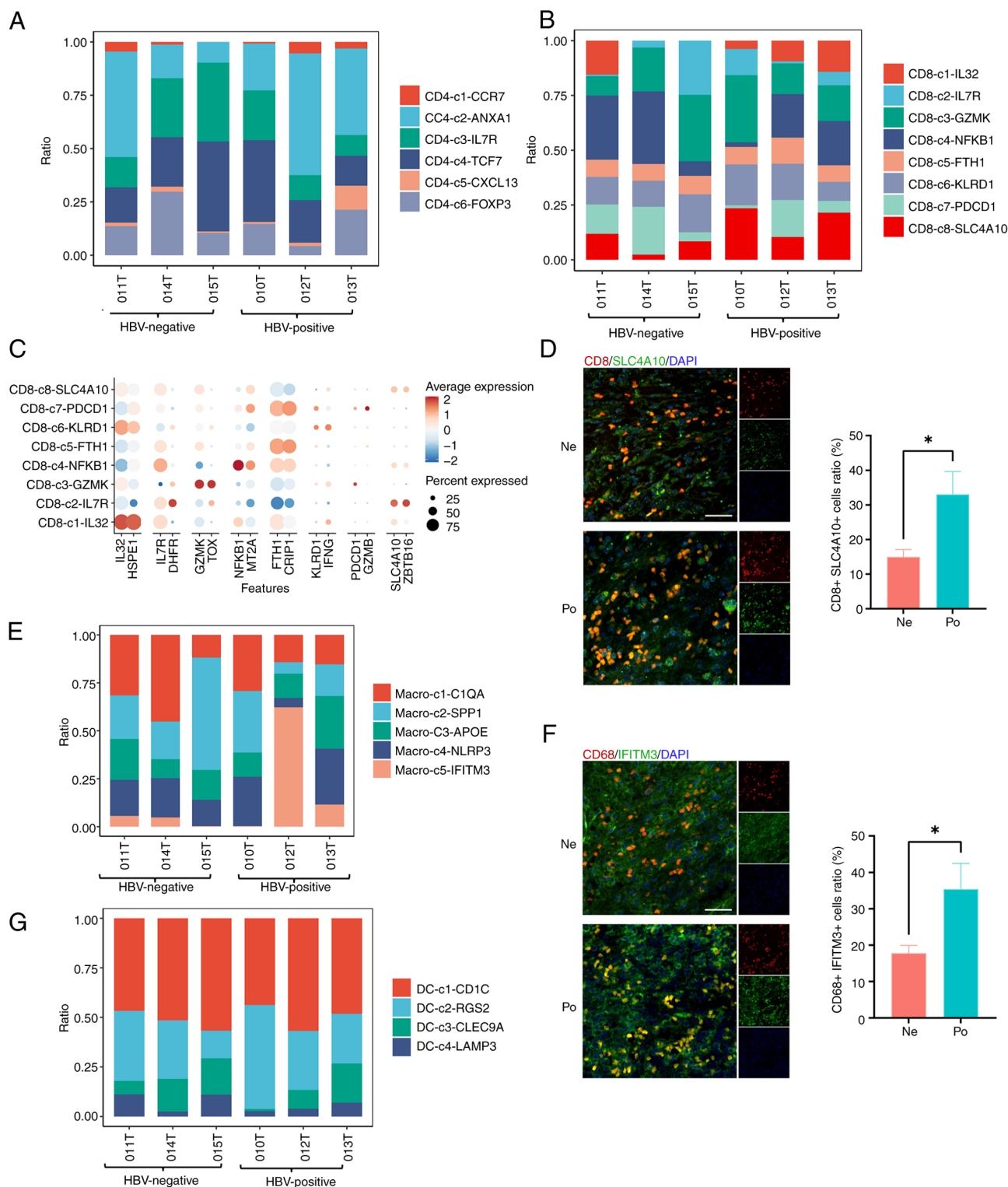


Figure S5. Effect of HBV infection on intercellular communication within tumor liver tissues across all identified cell subtypes. Increased intercellular communication is represented in red, whereas decreased communication is shown in blue. HBV, hepatitis B virus.

